**Electronic Supplementary Information for:**

# Trapping an Unusual Pentacoordinate Carbon Atom in a Neutral Trialuminum Complex

*Nery Villegas-Escobar[1,]*, Javier Martínez[2,], Ricardo A. Matute[1,3], Sebastián Saltarini[4], Constantin G. Daniliuc[5], Lutz Gade[6], and René S. Rojas[4]**

[1]Centro Integrativo de Biología y Química Aplicada (CIBQA) Universidad Bernardo O'Higgins, General Gana 1702, Santiago 8370854, Chile

[2]Instituto de Ciencias Químicas, Facultad de Ciencias, Isla Teja, Universidad Austral de Chile, 5090000 Valdivia, Chile.

[3]Division of Chemistry and Chemical Engineering, California Institute of Technology, Pasadena, CA.

[4]Laboratorio de Química Inorgánica, Facultad de Química y Farmacia, Pontificia Universidad Católica de Chile, Santiago 6094411, Chile.

[5]Organisch-Chemisches Institut der Universität Münster, 48149 Münster, Germany

[6]Anorganisch-Chemisches Institut, Universität Heidelberg, Im Neuenheimer Feld 270, 69120 Heidelberg, Germany

nery.villegas@ubo.cl, rrojasg@uc.cl

## TABLE OF CONTENTS

## Experimental Section

All the reagents were purchased from commercial sources, unless otherwise specified and used as received. NMR spectra were recorded on an NMR Bruker AV 400 instrument. Chemical shifts are given in parts per million relative to TMS [$^{1}$H and $^{13}$C, δ($SiMe_4$) = 0] or an external standard. Most NMR assignments were supported by additional 2D experiments. HRMS-ESI-MS experiments were performed using a Thermo Scientific Exactive Plus Orbitrap spectrometer

## Synthesis of complex 1

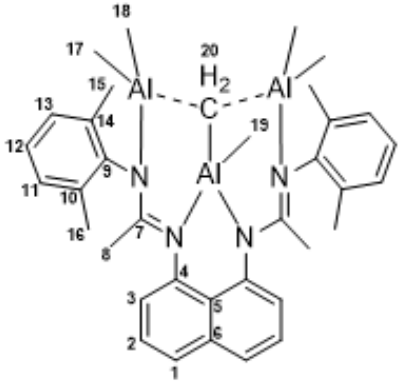


A solution of **L1** (100.0 mg, 0.22 mmol) was added to a solution of trimethylaluminum (TMA) (49.8 mg, 0.69 mmol), both in dry dichloromethane. The reaction mixture was stirred for 2 h at room temperature under a nitrogen atmosphere. After that, all volatiles were removed under a vacuum. The crude product was washed in anhydrous hexane and recrystallised from a concentrated solution in dry dichloromethane by toluene vapour diffusion into the solid. Compound **1** was obtained as pale orange crystals (116.3 mg, 85 %).

**$^{1}$H NMR** (400 MHz, $CDCl_3$) δ/ppm = 7.68 (d, *J* = 8.4 Hz, 2H, $H_3$), 7.42 (t, *J* = 8.4 Hz, 2H, $H_2$), 7.18 (t, J = 4.4 Hz, 2H, $H_{12}$), 7.10 (d, J = 5,2 Hz, 4H, $H_{11,13}$), 6.86 (d, J = 7.2 Hz, 2H, $H_1$), 2.39 (s, 6H, $H_{15}$), 2.25 (s, 6H, $H_{16}$), 1.86 (s, 6H, $H_8$), 0.26 (brs, 2H, $H_{20}$) –0.52 (s, 6H, $H_{17,18}$), –1.11 (s, 3H, $H_{19}$), –1.21 ppm (s, 6H, $H_{17,18}$).

**$^{13}$C{$^{1}$H} NMR** (100 MHz, $CDCl_3$) δ/ppm = 170.95 ($C_7$), 143.77–132.81 ($C_{4–6,9,10,14}$), 129.01 ($C_{12}$), 128.24 ($C_{11,13}$), 126.03 ($C_{11,13}$), 125.82 ($C_2$), 125.60 ($C_3$), 123.74 ($C_1$), 21.14 ($C_8$), 20.10 ($C_{16}$), 18.91 ($C_{15}$), –0.56 ($C_{20}$), –4.17 ($C_{19}$),–6.18 ($C_{17,18}$), –7.44 ppm ($C_{17,18}$).

**HRMS (ESI):** m/z $[M+H]^+$ for $C_{36}H_{47}Al_3N_4$: calc: 617,733; found: 617.294.

**Figure S1.** $^{1}$H-NMR spectrum of complex **1** in $CDCl_3$.

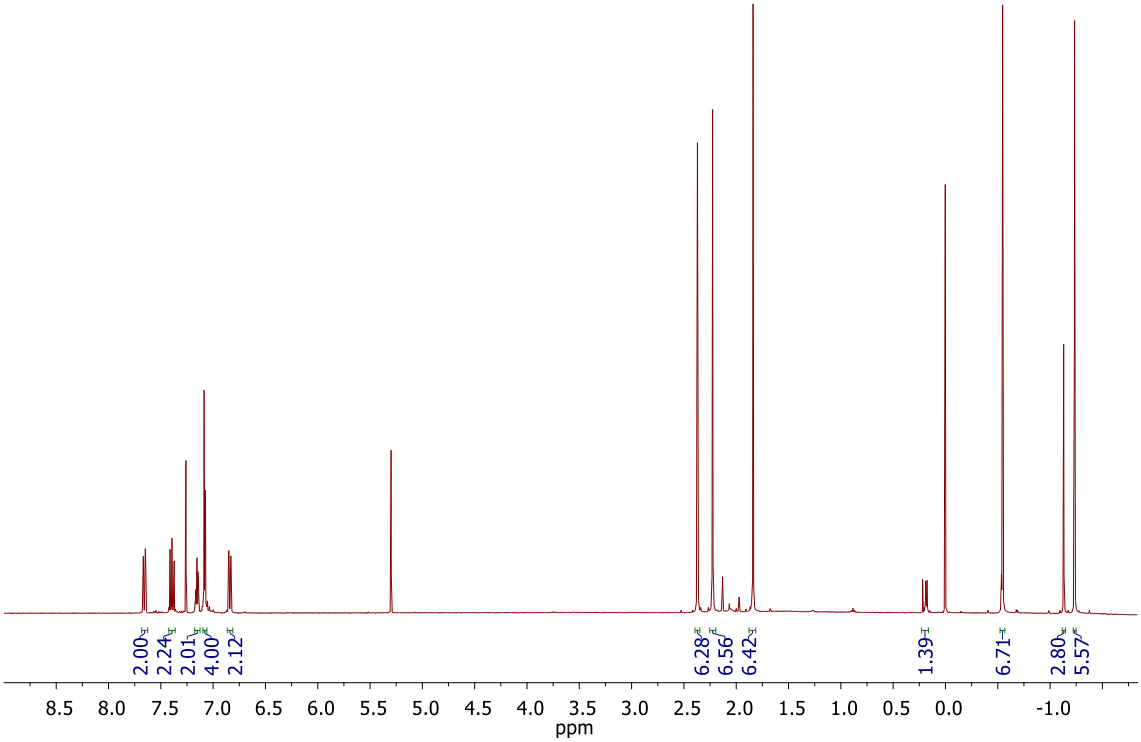


**Figure S2.** $^{1}$H-NMR spectrum of complex **1** in $CDCl_3$ (region 8.0-4.4 ppm).

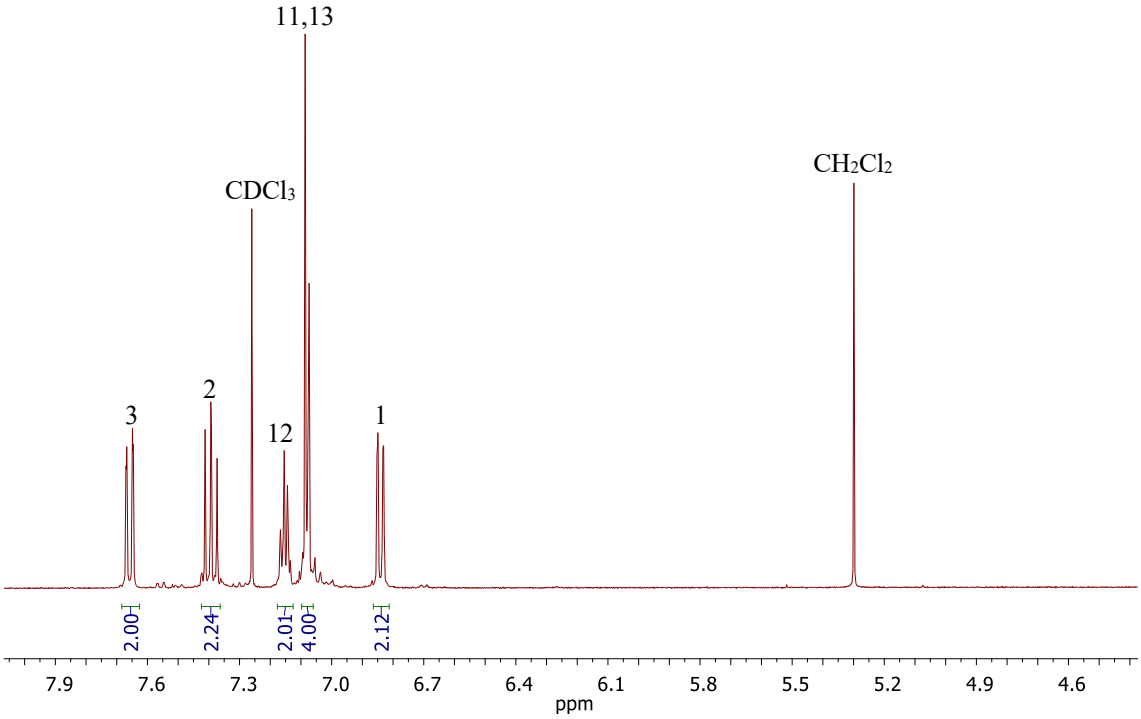

**Figure S3.** $^{1}$H-NMR spectrum of complex **1** in $CDCl_3$ (region 3.0-(−1.5) ppm).

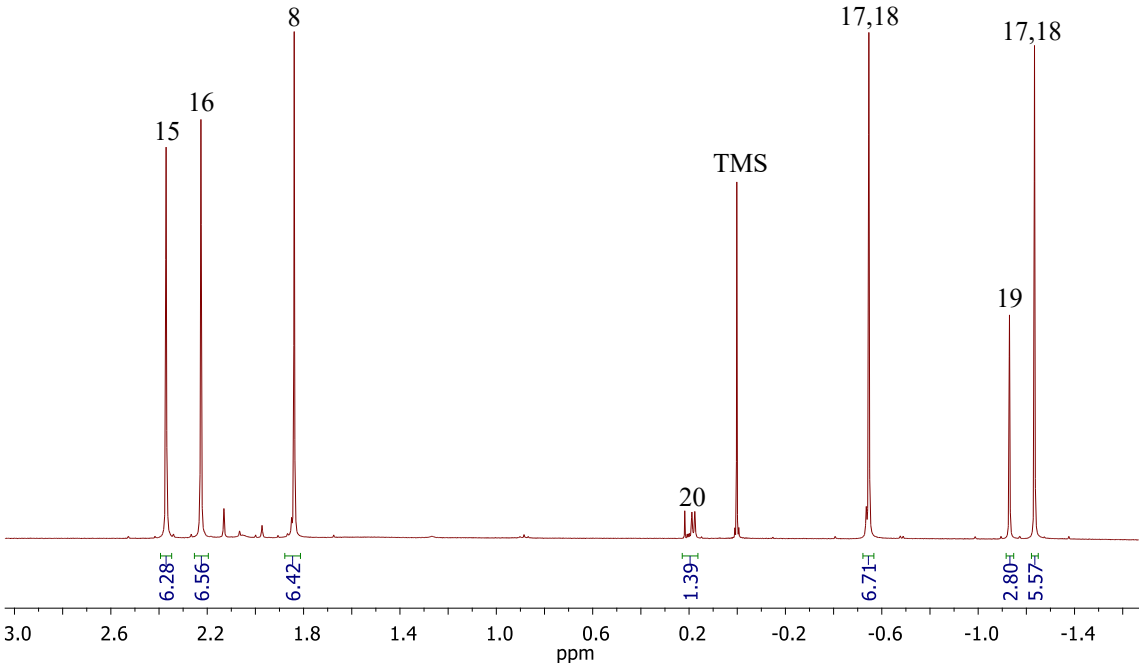


**Figure S4.** $^{13}$C{$^{1}$H}-NMR spectrum of complex **1** in $CDCl_3$.

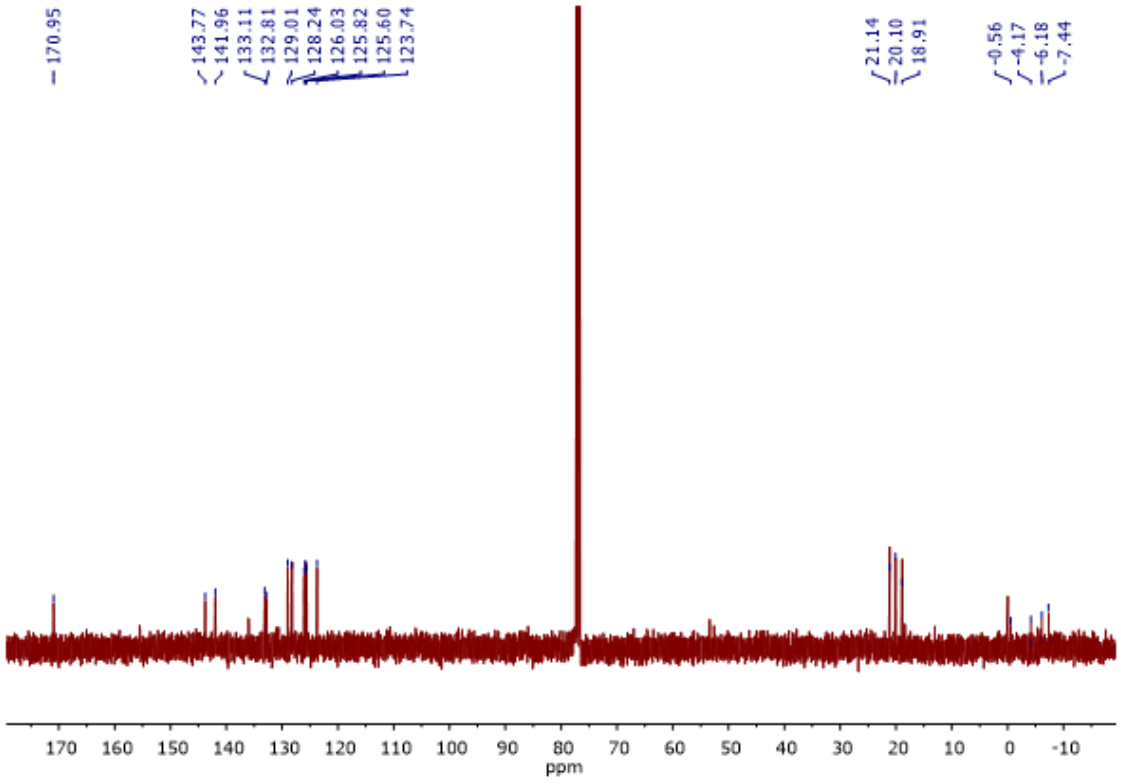

**Figure S5.** $^{1}H-^{13}C$ g-HSQC spectrum of complex **1**.

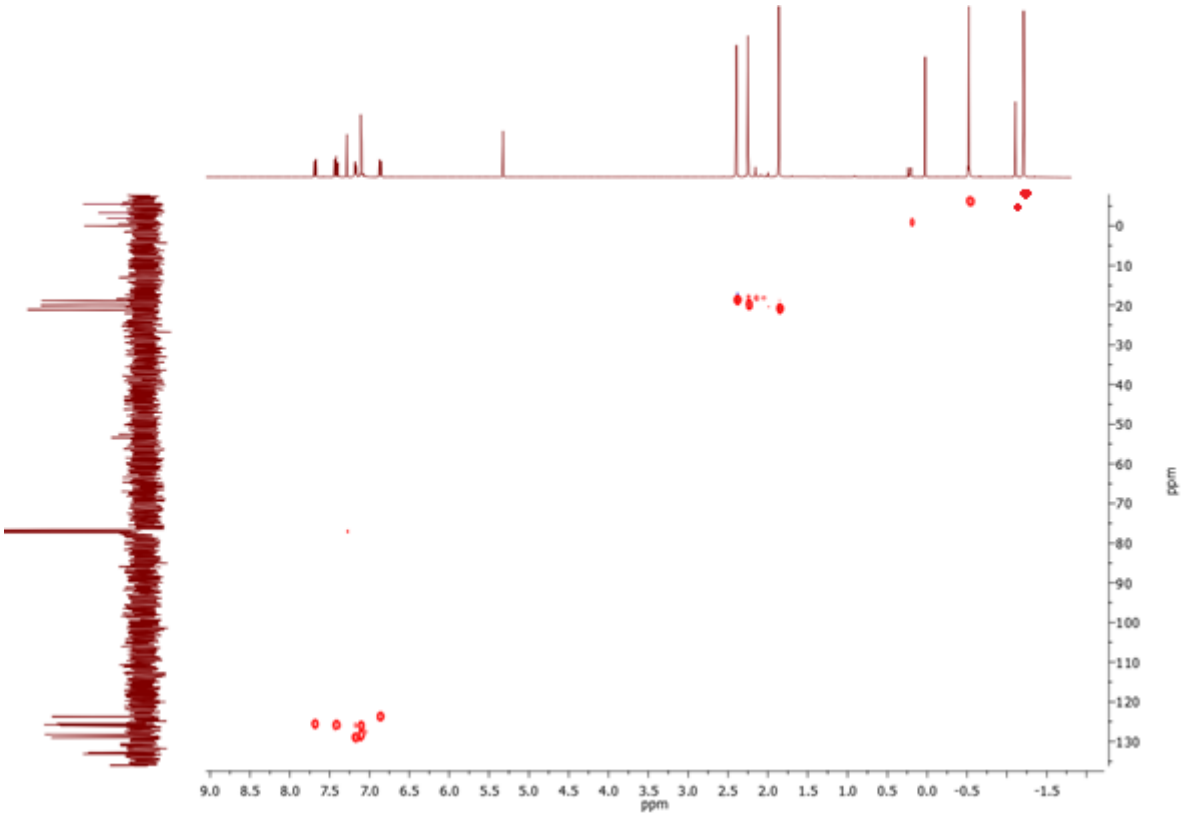


**Figure S6.** HRMS (ESI): m/z $[M+H]^{+}$ for complex **1**.

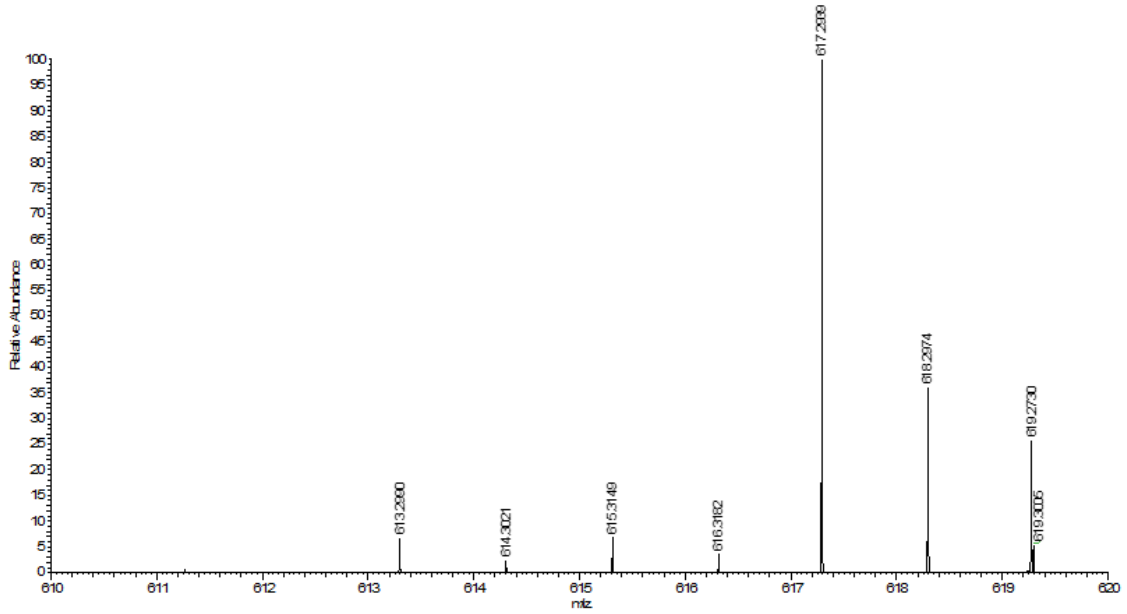

## X-ray diffraction studies

Data sets for compound **1** were collected with a Bruker D8 Venture PHOTON 100 diffractometer. Programs used: data collection, APEX3 V2016.1-0; cell refinement, SAINT V8.37A; data reduction: SAINT V8.37A; absorption correction, SADABS V2014/7;[1] structure solution SHELXT-2015;[2] structure refinement SHELXL-2015;[3] and graphics, XP.[4] R-values are given for observed reflections, and $wR^2$ values are given for all reflections.

Exceptions and unique features: For compound **1,** one disordered over two positions dichloromethane molecule was found in the asymmetrical unit. Several restraints (SADI, SAME, ISOR and SIMU) were used to improve refinement stability.

The hydrogens at the C9 atom were refined freely. CCDC Nr.: **2074776**.

**Figure S7.** Crystal structure of compound **1**. (Thermal ellipsoids are shown with 30% probability.)

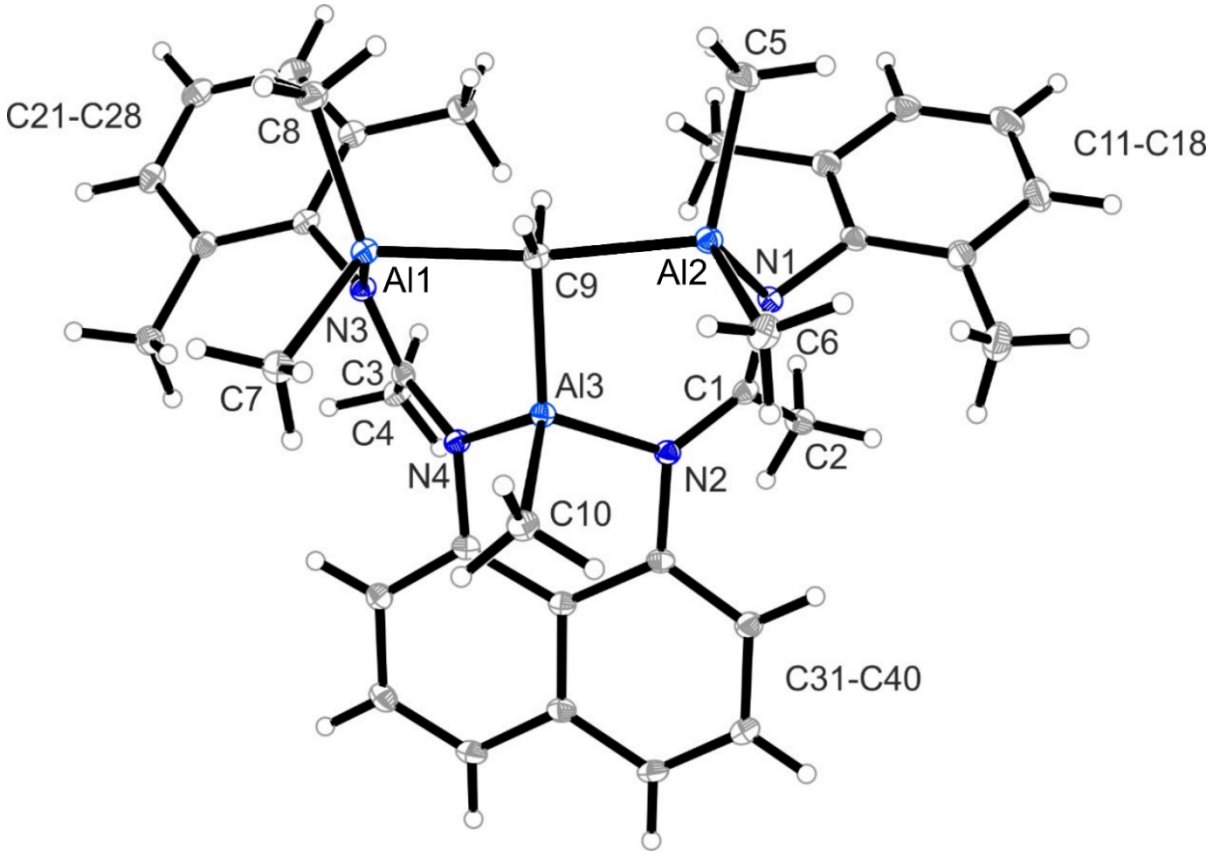

**Table S1.** Crystallographic data and structure refinement of complex **1**.

| | **1** |
|---|---|
| Empirical formula | $C_{37}H_{49}Al_3Cl_2N_4$ |
| Formula weight | 701.663 g/mol |
| Temperature (K) | 102(2) |
| Wavelength (Å) | 1.54178 |
| Crystal system | monoclinic |
| Space group | $P2_1/n$ |
| a(Å) | 9.7351(2) |
| b(Å) | 34.9337(7) |
| c(Å) | 11.2629(2) |
| α(º) | 90 |
| β(º) | 95.4670(10) |
| γ(º) | 90 |
| Volume(Å$^3$) | 3812.90(13) |
| Z | 4 |
| Density (calculated) (g/cm$^3$) | 1.222 |
| Absorption coefficient (mm$^{-1}$) | 2.433 |
| F(000) | 1488 |
| Crystal size (mm$^3$) | 0.055 x 0.066 x 0.114 |
| Index ranges | $-11 \leq h \leq 11$<br>$-41 \leq k \leq 42$<br>$-12 \leq l \leq 13$ |
| Reflections collected | 54025 |
| Independent reflections | 6967 [R(int) = 0.0508] |
| Data/restraints/parameters | 6967 / 49 / 453 |
| Goodness-of-fit on $F^2$ | 1.082 |
| Final R indices [I>2σ(I)] | R1 = 0.0399,<br>wR2 = 0.0995 |
| R indices (all data) | R1 = 0.0466<br>wR2 = 0.1032 |
| Largest diff. peak/hole, e.Å$^{-3}$ | 0.312 and –0.370 |

**Table S2.** Principal bond distances (Å) for complex **1**.

| **1 (Bond distances, Å)** | | | |
|---|---|---|---|
| Al1–N1 | 1.951(17) | Al1–C6 | 1.966(2) |
| Al1–C5 | 1.974(2) | Al1–C9 | 2.098(2) |
| Al1–Al3 | 2.979(8) | Al2–N3 | 1.948(16) |
| Al2–C8 | 1.966(2) | Al2–C7 | 1.970(2) |
| Al2–C9 | 2.100(2) | Al2–Al3 | 2.932(8) |
| Al3–N4 | 1.921(16) | Al3–N2 | 1.923(16) |
| Al3–C10 | 1.951(2) | **Al3–C9** | **1.958(2)** |
| N1–C1 | 1.326(2) | N1–C11 | 1.449(2) |
| N2–C1 | 1.343(2) | N2–C31 | 1.432(2) |
| N3–C3 | 1.318(2) | N3–C21 | 1.450(2) |
| N4–C3 | 1.351(2) | N4–C39 | 1.422(2) |
| C1–C2 | 1.509(3) | C2–H2A | 0.98 |
| C2–H2B | 0.98 | C2–H2C | 0.98 |
| C3–C4 | 1.509(3) | C4–H4A | 0.98 |
| C4–H4B | 0.98 | C4–H4C | 0.98 |
| C5–H5A | 0.98 | C5–H5B | 0.98 |
| C5–H5C | 0.98 | C6–H6A | 0.98 |
| C6–H6B | 0.98 | C6–H6C | 0.98 |
| C7–H7A | 0.98 | C7–H7B | 0.98 |
| C7–H7C | 0.98 | C8–H8A | 0.98 |
| C8–H8B | 0.98 | C8–H8C | 0.98 |
| C9–H9A | 0.95(3) | C9–H9B | 0.90(3) |
| C10–H10A | 0.98 | C10–H10B | 0.98 |
| C10–H10C | 0.98 | C11–C12 | 1.399(3) |
| C11–C16 | 1.402(3) | C12–C13 | 1.396(3) |
| C12–C17 | 1.509(3) | C13–C14 | 1.384(3) |
| C13–H13 | 0.95 | C14–C15 | 1.381(3) |

**Table S3.** Principal bond angles (º) for complex **1**.

| **1 (Bond angles, º)** | | | |
|---|---|---|---|
| N1–Al1–C6 | 107.29(8) | N1–Al1–C5 | 109.28(8) |
| Al1–C9– Al2 | 173.10(11) | Al3–C9– Al1 | 94.47(8) |
| C6–Al1–C5 | 116.55(9) | N1–Al1–C9 | 105.50(7) |
| C6–Al1–C9 | 107.03(8) | C5–Al1–C9 | 110.59(9) |
| N1–Al1–Al3 | 80.81(5) | C6–Al1–Al3 | 146.78(7) |
| C5–Al1–Al3 | 89.24(7) | C9–Al1–Al3 | 40.95(5) |
| N3–Al2–C8 | 109.14(8) | N3–Al2–C7 | 108.19(8) |
| C8–Al2–C7 | 115.58(9) | N3–Al2–C9 | 101.19(7) |
| C8–Al2-C9 | 108.51(8) | C7-Al2-C9 | 113.21(8) |
| N3–Al2–Al3 | 82.41(5) | C8–Al2–Al3 | 150.38(7) |
| C7–Al2–Al3 | 84.46(6) | C9–Al2–Al3 | 41.87(5) |
| N4–Al3–N2 | 89.75(7) | N4–Al3–C10 | 114.23(8) |
| N2–Al3–C10 | 108.88(8) | N4–Al3–C9 | 109.55(8) |
| N2–Al3–C9 | 113.23(8) | C10–Al3–C9 | 117.83(9) |
| N4–Al3–Al2 | 75.42(5) | N2–Al3–Al2 | 142.84(5) |
| C10–Al3–Al2 | 108.27(7) | C9–Al3–Al2 | 45.71(6) |
| N4–Al3–Al1 | 135.85(5) | N2–Al3–Al1 | 76.83(5) |
| C10–Al3–Al1 | 109.91(7) | C9–Al3–Al1 | 44.59(6) |
| Al2–Al3–Al1 | 90.30(2) | C1–N1–C11 | 117.53(15) |
| C1–N1–Al1 | 125.70(13) | C11–N1–Al1 | 116.53(12) |
| C1–N2–C31 | 119.72(15) | C1–N2–Al3 | 130.02(13) |
| C31–N2–Al3 | 110.01(12) | C3–N3–C21 | 119.25(15) |
| C3–N3–Al2 | 123.07(13) | C21–N3–Al2 | 117.36(11) |
| C3–N4–C39 | 118.66(15) | C3–N4–Al3 | 129.64(13) |
| C39–N4–Al3 | 111.48(12) | N1–C1–N2 | 119.51(17) |
| N1–C1–C2 | 119.12(17) | N2–C1–C2 | 121.27(16) |
| C1–C2–H2A | 109.5 | C1–C2–H2B | 109.5 |
| H2A–C2–H2B | 109.5 | C1–C2–H2C | 109.5 |
| H2A–C2–H2C | 109.5 | H2B–C2–H2C | 109.5 |

## Computational Section

Optimisation of complex **1** was obtained using density functional theory (DFT), employing the wB97XD exchange-correlation functional[5,6] together with the def2-TZVPP basis set.[7] All calculations were performed using the Gaussian16 (RevB.01) software package.[8] Mayer bond order, natural charges, and donor-acceptor second-order perturbation energies were obtained in the natural bond orbital (NBO) basis using the NBO 3.1 software interfaced with Gaussian16. Noncovalent interactions (NCIs) were revealed using the NCI index proposed by Johnson and coworkers through the NCIplot software.[9,10] A wavefunction file was generated in Gaussian16 to be used as input for the NCIplot program. Atoms in Molecules (AIM)[11–15] analyses and adaptive natural density partitioning (AdNDP)[16] were performed in Multiwfn[17] using the .wfn generated in Gaussian.

Molecular dynamic simulations were performed using the atom-centred density matrix propagation (ADMP) procedure[18–20] as implemented in Gaussian16. The dynamic was propagated with a total of 20,000 conformations in a total time of 2.0 ps (2.000 fs) at the wB97XD/6-31G level of theory. Bond distance distributions were computed in Gabedit[21] using the radial pair distribution function.

## Computational Results

**Table S4.** Comparison between crystal and optimised structures.

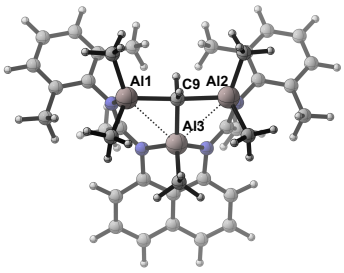


| Bond | Crystal | M06-2X | *w*B97XD | BO Wiberg | BO Mayer |
|---|---|---|---|---|---|
| Al1-C9 | 2.098(2) | 2.101 | 2.09696 | 0.3287 | 0.4357 |
| Al2-C9 | 2.100(2) | 2.101 | 2.097 | 0.3287 | 0.4357 |
| Al3-C9 | 1.958(2) | 1.974 | 1.973 | 0.4113 | 0.5501 |
| Al1-C9-Al2 | 173.10(11) | 173.27 | 173.26 | -- | -- |

**Table S5.** Comparison of other Al–C bond distances in similar $Al_3$-($\mu^3$-$CH_2$) moieties.

| System | Al–C | Al–C | Al–C | Ref |
|---|---|---|---|---|
| **4,** [(Cp*Zr)$_3$Al$_6$Me$_8$(CH)$_5$(CH$_2$)$_2$] | **2.028(7)** Al1–C10 | **2.128(6)** Al2–C10 | **2.003(7)** Al4–C10 | 22 |
| **11,** [(Cp*Hf)$_3$Al$_6$Me$_8$($\mu^3$-CH$_2$)$_2$($\mu^4$-CH)$_4$($\mu^3$-CH)] | **2.071(8)** Al2–C7 | **2.063(8)** Al5–C7 | **2.047(8)** Al6–C7 | 23 |
| **2,** [Cp*$_2$UAl$_3$($\mu^3$-CH$_2$)($\mu^2$-CH$_3$)$_2$(CH$_3$)$_7$] | **2.076(6)** Al1–C25 | **2.018(6)** Al2–C25 | **2.104(6)** Al3–C25 | 24 |
| **4,** Me$_3$Al($\mu^3$-CH$_2$)(AlMe$_2$)$_2$($\mu^2$-CH$_3$)$^-$ | **2.061(3)** Al1–C17 | **1.991(3)** Al2–C17 | **2.128(3)** Al3–C17 | 25 |
| Me$_3$Al($\mu^3$-CH$_2$)(AlMe$_2$)$_2$($\mu^2$-CH$_3$)$^-$ | **2.081** Al1–C9 | **2.007** Al2–C9 | **2.125** Al3–C9 | 26 |
| **This work** | **2.098(2)** Al1–C9 | **2.100(2)** Al2–C9 | **1.958(2)** Al3–C9 | |

## QTAIM

Topological analysis based on the quantum theory of atoms in molecules (QTAIM)[11–15] was used to expose the formation of the pentacoordinate carbon atom. The Bond critical points (BCPs), density at the BCPs, and Mayer bond orders are shown for discussions in Figure S5. In contrast, density and Laplacian of the electron density are quoted in Figure S6. Although BCPs have been somewhat questioned in the hunt for covalent bonds,[27,28] the appearance of five BCPs and five bond paths around carbon reveals its pentacoordinate. Mainly, BCPs for the C–H bonds show large electron densities (~0.26 a.u.), typical for 2e-covalent bonds, with bond orders larger than 0.7.

Moreover, the negative values from the Laplacian of the electron density at the C–H BCPs corroborate the full covalent nature of these interactions (see Figure S6). Conversely, Although BCPs were observed for the Al–C contacts, the low electron density and positive values for the Laplacian of the electron density at the BCPs reveal that these interactions are dominated by an essential electrostatic contribution. However, the QTAIM results show that the Al3–C bond is inherently different from the Al1–C with the Al2–C bonds. A higher covalency is observed for the former by a more significant electron density (0.077 a.u.) found at the BCP and supported by a larger MBO= 0.550. Although long-range interactions were shown for the Al$^{\cdots}$Al contacts, no BCPs were found between these atoms. Nonetheless, ring critical points are observed in the two

6-membered C*–Al–N–C–N–Al rings, which are rather crucial in stabilising the methylidene moiety.

**Figure S8.** Laplacian of the electron density map and bond critical points (BCPs) in blue balls around the pentacoordinate carbon atom. Value of the density at BCPs (a.u.) and Mayer bond orders MBOs (in parenthesis).

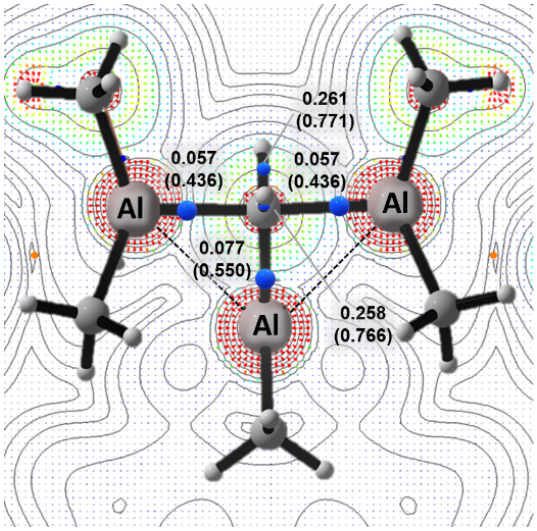


**Figure S9.** Key bond critical points (BCPs) on the molecular structure. Density and Laplacian of the electron density at each BCP. Values in atomic units (a.u.).

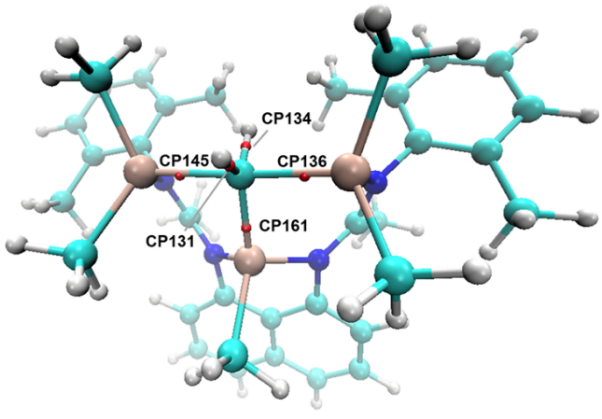


| Critical Point | ρ(r) | $\nabla^2\rho(r)$ |
|---|---|---|
| CP131 | 0.2576 | -0.8061 |
| CP134 | 0.2611 | -0.8314 |
| CP136 | 0.0571 | 0.1760 |
| CP145 | 0.0571 | 0.1760 |
| CP161 | 0.0769 | 0.2617 |

**Figure S10.** Bond and ring critical points together with bond paths are shown for complex **1**.

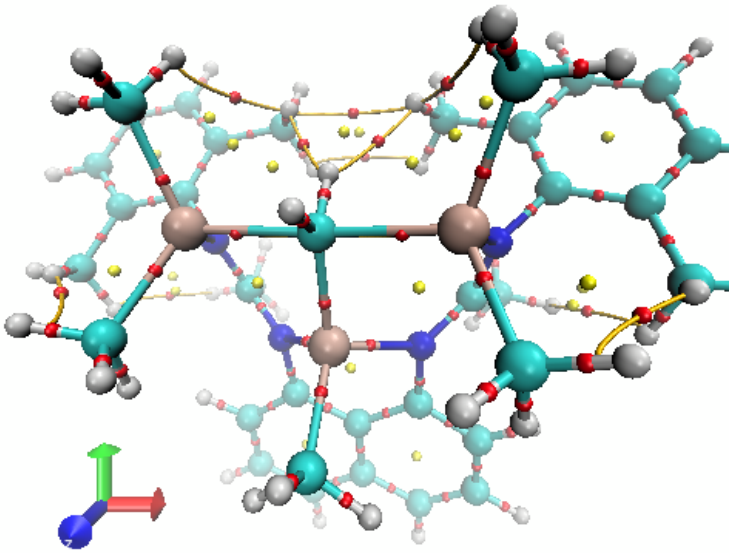

**Figure S11.** Superposition of molecular structures obtained at the wB97XD/6-31G and wB97XD/def2-TZVPP (quadrants). RMSD = 0.0372 (including hydrogens). The similarity of both structures supports the choice of the methodology for the dynamic simulation.

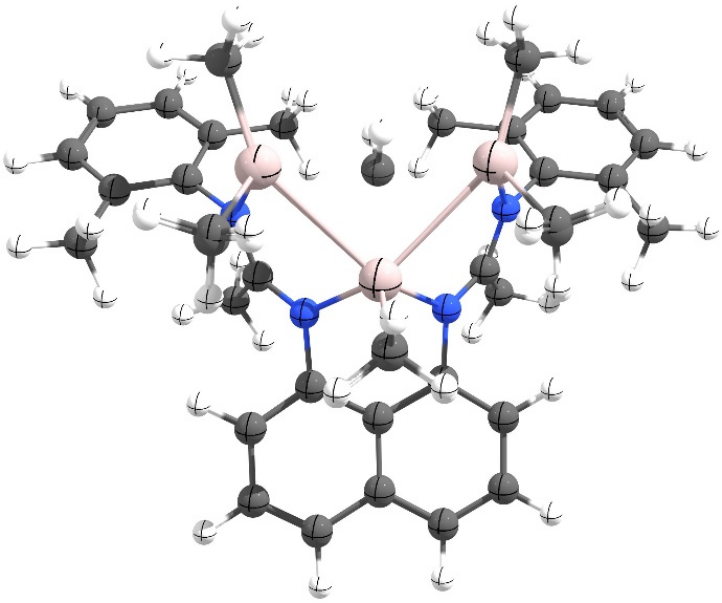

**Figure S12.** Results from trajectory. (a) total energy, (b) HOMO-LUMO gap, (c) HOMO energy (d) LUMO energy.

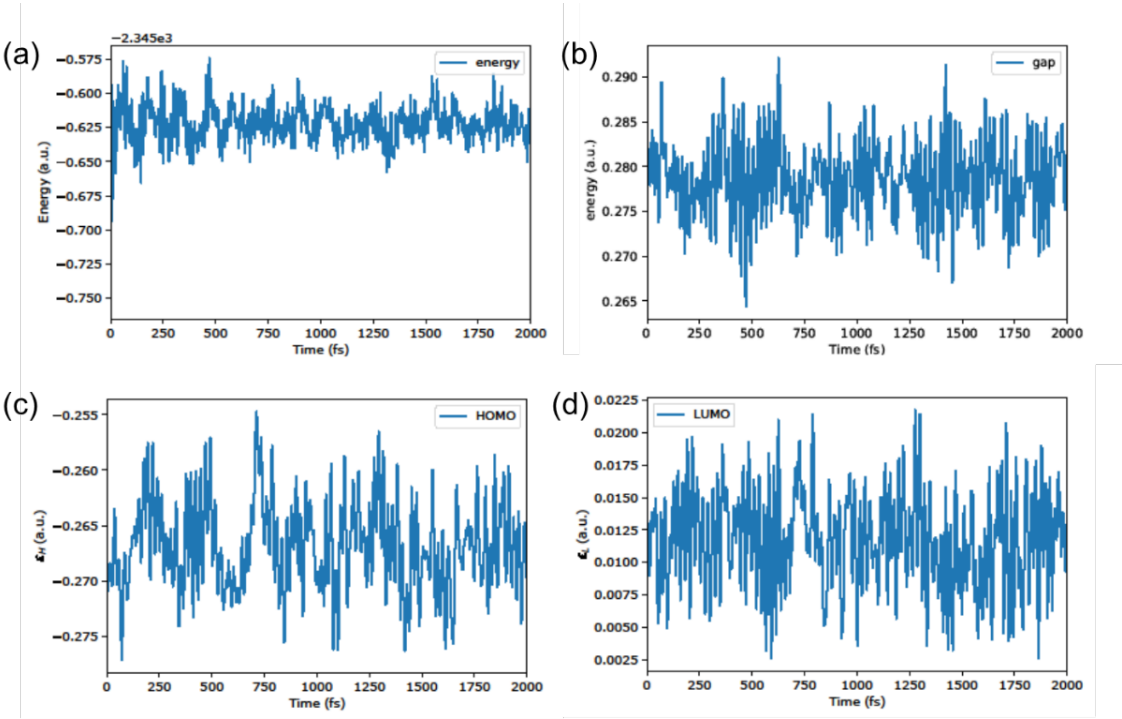

## XYZ coordinates

## wB97XD/def2TZVPP

Energy -2346.82916816 au

| | | | |
|---|---|---|---|
| Al | 2.090723 | -1.112903 | 1.871317 |
| Al | -2.090820 | -1.112843 | 1.871341 |
| Al | -0.000008 | 0.876803 | 1.338150 |
| N | 2.614161 | -0.645103 | 0.041250 |
| N | 1.353121 | 1.271894 | 0.010343 |
| N | -2.614231 | -0.645006 | 0.041270 |
| N | -1.353118 | 1.271946 | 0.010343 |
| C | 2.237871 | 0.458892 | -0.571673 |
| C | 2.760087 | 0.746382 | -1.956805 |
| H | 3.816625 | 1.010835 | -1.937744 |
| H | 2.209034 | 1.550742 | -2.431030 |
| H | 2.676040 | -0.158801 | -2.555954 |
| C | -2.237873 | 0.458950 | -0.571679 |
| C | -2.759955 | 0.746345 | -1.956884 |
| H | -2.675893 | -0.158897 | -2.555942 |
| H | -2.208820 | 1.550634 | -2.431131 |
| H | -3.816480 | 1.010849 | -1.937947 |
| C | 2.811238 | 0.269306 | 3.086488 |
| H | 3.808101 | -0.016614 | 3.435816 |
| H | 2.194760 | 0.399131 | 3.979849 |
| H | 2.903283 | 1.256363 | 2.625642 |
| C | 2.640057 | -2.976952 | 2.168588 |
| H | 2.196349 | -3.688719 | 1.467428 |
| H | 2.360985 | -3.308306 | 3.173297 |
| H | 3.724830 | -3.093093 | 2.088463 |
| C | -2.811255 | 0.269330 | 3.086584 |
| H | -2.902214 | 1.256716 | 2.626231 |
| H | -2.195340 | 0.398175 | 3.980479 |
| H | -3.808590 | -0.016011 | 3.435038 |
| C | -2.640230 | -2.976864 | 2.168648 |
| H | -3.725017 | -3.092934 | 2.088620 |
| H | -2.361090 | -3.308234 | 3.173333 |
| H | -2.196635 | -3.688665 | 1.467453 |
| C | -0.000047 | -1.039866 | 1.783668 |
| H | -0.000046 | -1.433854 | 2.808499 |
| H | -0.000068 | -1.878568 | 1.081236 |
| C | 0.000105 | 2.224408 | 2.750397 |
| H | -0.879844 | 2.869458 | 2.693786 |
| H | 0.881319 | 2.867838 | 2.695119 |
| H | -0.001077 | 1.768574 | 3.742463 |
| C | 3.572033 | -1.502155 | -0.587386 |
| C | 4.933287 | -1.260130 | -0.385533 |
| C | 5.852358 | -2.129698 | -0.960260 |
| H | 6.909950 | -1.953367 | -0.809527 |
| C | 5.434803 | -3.214648 | -1.710669 |
| H | 6.163276 | -3.884246 | -2.147948 |
| C | 4.082727 | -3.443833 | -1.894635 |
| H | 3.752319 | -4.295167 | -2.476336 |
| C | 3.135610 | -2.596492 | -1.335101 |
| C | 5.398097 | -0.098247 | 0.446084 |
| H | 5.033309 | 0.854185 | 0.057032 |
| H | 6.485295 | -0.054572 | 0.472356 |
| H | 5.034578 | -0.172266 | 1.471195 |
| C | 1.669944 | -2.846363 | -1.520347 |
| H | 1.494845 | -3.693272 | -2.181279 |
| H | 1.163990 | -1.976156 | -1.940742 |
| H | 1.190365 | -3.058880 | -0.564079 |
| C | -3.572088 | -1.502054 | -0.587399 |
| C | -4.933350 | -1.260065 | -0.385548 |
| C | -5.852397 | -2.129640 | -0.960301 |
| H | -6.909994 | -1.953346 | -0.809556 |
| C | -5.434813 | -3.214552 | -1.710749 |
| H | -6.163268 | -3.884155 | -2.148049 |
| C | -4.082732 | -3.443691 | -1.894728 |
| H | -3.752301 | -4.294988 | -2.476470 |
| C | -3.135637 | -2.596348 | -1.335160 |
| C | -5.398198 | -0.098223 | 0.446108 |
| H | -5.034534 | -0.172169 | 1.471169 |
| H | -6.485399 | -0.054684 | 0.472518 |
| H | -5.033589 | 0.854247 | 0.056981 |
| C | -1.669965 | -2.846161 | -1.520445 |
| H | -1.190392 | -3.058877 | -0.564219 |
| H | -1.164021 | -1.975857 | -1.940649 |
| H | -1.494849 | -3.692929 | -2.181553 |
| C | 1.268768 | 2.625704 | -0.389833 |
| C | 2.423756 | 3.361397 | -0.499181 |

H 3.366880 2.878228 -0.282192
C 2.408571 4.714633 -0.860666
H 3.342386 5.252776 -0.951994
C 1.220700 5.345811 -1.068580
H 1.189292 6.394161 -1.334658
C 0.000073 4.652120 -0.906410
C -1.220526 5.345853 -1.068617
H -1.189073 6.394202 -1.334692
C -2.408424 4.714718 -0.860733
H -3.342218 5.252892 -0.952086
C -2.423666 3.361482 -0.499242
H -3.366812 2.878354 -0.282263
C -1.268709 2.625745 -0.389867
C 0.000043 3.268145 -0.566286

## wB97XD/6-31G

Energy -2345.75598279 au
Al 2.130197 -1.097247 1.892885
Al -2.130137 -1.097298 1.892891
Al 0.000008 0.881331 1.353569
N 2.629713 -0.651418 0.035072
N 1.358845 1.286476 -0.005873
N -2.629692 -0.651456 0.035091
N -1.358853 1.286452 -0.005855
C 2.246919 0.461005 -0.591431
C 2.777561 0.741888 -1.981800
H 3.841048 0.997478 -1.964165
H 2.232750 1.554610 -2.458503
H 2.681175 -0.163374 -2.587302
C -2.246923 0.460981 -0.591406
C -2.777663 0.741980 -1.981713
H -2.681309 -0.163219 -2.587312
H -2.232896 1.554759 -2.458372
H -3.841152 0.997559 -1.963977
C 2.837132 0.344878 3.073626
H 3.817948 0.056432 3.476599
H 2.178631 0.534549 3.931030
H 2.960883 1.298141 2.542765
C 2.689435 -2.971861 2.207506
H 2.240297 -3.674048 1.493012
H 2.403515 -3.300312 3.215972
H 3.779440 -3.077793 2.123203
C -2.837084 0.344800 3.073658
H -2.960874 1.298061 2.542803
H -2.178566 0.534487 3.931046
H -3.817883 0.056328 3.476656
C -2.689317 -2.971931 2.207500
H -3.779320 -3.077898 2.123207
H -2.403376 -3.300379 3.215960
H -2.240163 -3.674097 1.492995
C 0.000030 -1.042281 1.815900
H 0.000033 -1.422670 2.851731
H 0.000040 -1.880564 1.105352
C 0.000001 2.286522 2.733648
H -0.887561 2.924881 2.643181
H 0.887544 2.924907 2.643166
H 0.000016 1.860339 3.743448
C 3.587193 -1.529660 -0.586818
C 4.958727 -1.297685 -0.379802
C 5.878085 -2.187350 -0.945944
H 6.939181 -2.019588 -0.791088
C 5.448591 -3.281690 -1.693374
H 6.173709 -3.964385 -2.122399
C 4.086183 -3.500797 -1.883114
H 3.747920 -4.356360 -2.459001
C 3.139331 -2.632623 -1.331315
C 5.430096 -0.130088 0.451709
H 5.042863 0.824799 0.078196
H 6.521649 -0.072783 0.454212
H 5.091329 -0.218206 1.489114
C 1.664947 -2.869740 -1.515230
H 1.480079 -3.725350 -2.170081
H 1.165156 -1.995451 -1.946589
H 1.182141 -3.068146 -0.552449
C -3.587172 -1.529713 -0.586780
C -4.958707 -1.297707 -0.379805
C -5.878067 -2.187387 -0.945923
H -6.939164 -2.019599 -0.791103
C -5.448573 -3.281774 -1.693284
H -6.173691 -3.964480 -2.122289
C -4.086163 -3.500914 -1.882979
H -3.747901 -4.356515 -2.458808

| | | | |
|---|---|---|---|
| C | -3.139311 | -2.632725 | -1.331204 |
| C | -5.430078 | -0.130055 | 0.451625 |
| H | -5.091388 | -0.218148 | 1.489057 |
| H | -6.521629 | -0.072696 | 0.454050 |
| H | -5.042772 | 0.824798 | 0.078100 |
| C | -1.664925 | -2.869887 | -1.515058 |
| H | -1.182143 | -3.068188 | -0.552245 |
| H | -1.165108 | -1.995658 | -1.946509 |
| H | -1.480058 | -3.725575 | -2.169807 |
| C | 1.273797 | 2.651861 | -0.406398 |
| C | 2.439938 | 3.386826 | -0.522446 |
| H | 3.384797 | 2.899474 | -0.308570 |
| C | 2.424698 | 4.749468 | -0.879615 |
| H | 3.361149 | 5.287390 | -0.973353 |
| C | 1.228116 | 5.387775 | -1.080170 |
| H | 1.196640 | 6.439994 | -1.342315 |
| C | -0.000051 | 4.691258 | -0.917895 |
| C | -1.228240 | 5.387726 | -1.080217 |
| H | -1.196796 | 6.439944 | -1.342370 |
| C | -2.424805 | 4.749371 | -0.879712 |
| H | -3.361275 | 5.287252 | -0.973497 |
| C | -2.440004 | 3.386733 | -0.522524 |
| H | -3.384851 | 2.899338 | -0.308687 |
| C | -1.273836 | 2.651826 | -0.406405 |
| C | -0.000028 | 3.297865 | -0.580243 |

## References


1. *APEX3* (**2016**), *SAINT* (**2015**) and *SADABS* (**2015**), Bruker AXS Inc., Madison, Wisconsin, USA.
2. G. M. Sheldrick, *SHELXT – Integrated space-group and crystal-structure determination*, *Acta Cryst.,* 2015, **A71**, 3-8.
3. G. M. Sheldrick, *Crystal structure refinement with SHELXL*, *Acta Cryst.*, 2015, **C71** *(1)*, 3-8.
4. *XP – Interactive molecular graphics, Version 5.1,* Bruker AXS Inc., Madison, Wisconsin, USA, **1998**.
5. J.-D. Chai and M. Head-Gordon, *J. Chem. Phys.*, 2008, **128**, 084106.
6. J.-D. Chai and M. Head-Gordon, *Phys. Chem. Chem. Phys.*, 2008, **10**, 6615.
7. T. H. Dunning, *J. Chem. Phys.*, 1989, **90**, 1007–1023.
8. V. M. Frisch, M. J.; Trucks, G. W.; Schlegel, H. B.; Scuseria, G. E.; Robb, M. A.; Cheeseman, J. R.; Scalmani, G.; Barone, M. . B.; Petersson, G. A.; Nakatsuji, H.; Caricato, M.; Li, X.; Hratchian, H. P.; Izmaylov, A. F.; Bloino, J.; Zheng, G.; Sonnenberg, J. L.; Hada, J. A. . Ehara, M.; Toyota, K.; Fukuda, R.; Hasegawa, J.; Ishida, M.; Nakajima, T.; Honda, Y.; Kitao, O.; Nakai, H.; Vreven, T.; Montgomery, Jr., J. . Peralta, J. E.; Ogliaro, F.; Bearpark, M. J.; Heyd, J.; Brothers, E. N.; Kudin, K. N.; Staroverov, V. N.; Kobayashi, R.; Normand, R. . Raghavachari, K.; Rendell, A. P.; Burant, J. C.; Iyengar, S. S.; Tomasi, J.; Cossi, M.; Rega, N.; Millam, N. J.; Klene, M.; Knox, J. E.; Cross, J. B.; Bakken, V.; Adamo, C.; Jaramillo, J.; Gomperts, V. G. . Stratmann, R. E.; Yazyev, O.; Austin, A. J.; Cammi, R.; Pomelli, C.;Ochterski, J. W.; Martin, R. L.; Morokuma, K.; Zakrzewski, A. Voth, G. A.; Salvador, P.; Dannenberg, J. J.; Dapprich, S.; Daniels and D. J. D.; Farkas, O.; Foresman, J. B.; Ortiz, J. V.; Cioslowski, J.; Fox, *Gaussian16 (Revision A.03)*, 2016.
9. E. R. Johnson, S. Keinan, P. Mori-Sánchez, J. Contreras-García, A. J. Cohen and W. Yang, *J. Am. Chem. Soc.*, 2010, **132**, 6498–6506.
10. J. Contreras-García, E. R. Johnson, S. Keinan, R. Chaudret, J.-P. Piquemal, D. N. Beratan and W. Yang, *J. Chem. Theory Comput.*, 2011, **7**, 625–632.
11. R. F. W. Bader, *Acc. Chem. Res.*, 1985, **18**, 9–15.
12. R. F. W. Bader, *In Atoms in Molecules: A Quantum Theory*, Oxford: Clarendon Press, 1990.
13. R. F. W. Bader, *Chem. Rev.*, 1991, **91**, 893–928.
14. H. J. Bohórquez, R. J. Boyd and C. F. Matta, *J. Phys. Chem. A*, 2011, **115**, 12991–12997.
15. P. S. V. KUMAR, V. RAGHAVENDRA and V. SUBRAMANIAN, *J. Chem. Sci.*, 2016,

**128**, 1527–1536.
16. D. Y. Zubarev and A. I. Boldyrev, *Phys. Chem. Chem. Phys.*, 2008, **10**, 5207–5217.
17. T. Lu and F. Chen, *J. Comput. Chem.*, 2012, **33**, 580–592.
18. S. S. Iyengar, H. B. Schlegel, J. M. Millam, G. A. Voth, G. E. Scuseria and M. J. Frisch, *J. Chem. Phys.*, 2001, **115**, 10291.
19. H. B. Schlegel, J. M. Millam, S. S. Iyengar, G. A. Voth, A. D. Daniels, G. E. Scuseria and M. J. Frisch, *J. Chem. Phys.*, 2001, **114**, 9758–9763.
20. H. B. Schlegel, S. S. Iyengar, X. Li, J. M. Millam, G. A. Voth, G. E. Scuseria and M. J. Frisch, *J. Chem. Phys.*, 2002, **117**, 8694–8704.
21. A.-R. Allouche, *J. Comput. Chem.*, 2011, **32**, 174–182.
22. A. Herzog, H. W. Roesky, Z. Zak and M. Noltemeyer, *Angew. Chemie Int. Ed. English*, 1994, **33**, 967–968.
23. A. Herzog, H. W. Roesky, F. Jäger, A. Steiner and M. Noltemeyer, *Organometallics*, 1996, **15**, 909–917.
24. H. M. Dietrich, J. W. Ziller, R. Anwander and W. J. Evans, *Organometallics,* 2009, **4**, 1173–1179.
25. A. L. Schmitt, G. Schnee, R. Welter and S. Dagorne, *Chem. Commun.*, 2010, **46**, 2480–2482.
26. G. Schnee, D. Specklin, J. P. Djukic and S. Dagorne, *Organometallics*, 2016, **35**, 1726–1734.
27. M. Jabłoński, *J. Comput. Chem.*, 2018, **39**, 2183–2195.
28. S. Shahbazian, *Chem. - A Eur. J.*, 2018, **24**, 5401–5405.